ELSEVIER

Magnetic Resonance Imaging 18 (2000) 615–624

MAGNETIC RESONANCE IMAGING

Finite size disc gradient coil set for open vertical field magnets

Labros S. Petropoulos*

USA Instruments Inc., 1515 Danner Drive, Aurora, OH 44202, USA

Received 15 November 1999; accepted 28 January 2000

Abstract

A new analytical approach is used in the design of disc-like gradient coils suitable for magnet geometries with main field direction perpendicular to the surface of the disc. An inverse procedure is used to optimize the coil's characteristics, subject to the restrictions imposed by the desired field behavior over a certain set of constraint points inside a predetermined imaging volume. Excellent agreement between the expected values of the gradient magnetic field and the numerical values generated by applying the Biot-Savart law to a discrete current pattern of the perspective disc coil was found. A Finite Element Analysis package was used to predict the fringe gradient field levels for a non-shielded axial disc coil and for a self-shielded transverse disc coil in the vicinity of the magnet poles. The numerical results indicate that for the self-shielded design the gradient fringe field is 1000 times smaller than the corresponding fringe field for the non-shielded disc case. Also no significant spatial dependence was noticed for the shielded coil's fringe field.

Keywords: Disc coil; Target field approach; Vertical field magnets; Self-shielded gradients; Non-shielded gradients; Eddy currents

1. Introduction

In the past few years, the trend towards faster high-resolution magnetic resonance imaging (MRI) sequences, such as 2D and 3D Echo Planar Imaging (EPI) and 2D and 3D Fast Spin Echo Imaging, has increased the demand for high strength and rapidly switched gradient fields. The philosophy behind the design of such gradient coils can, in general, be viewed as a convolution of two interrelated components. The first component focuses on the substantial improvement of the basic gradient field characteristics. In this case, improvements involving the gradient field's technical properties, such as the gradient strength, the required rise time to achieve the highest possible field strength, the slew rate and the gradient field linearity and uniformity over the desired imaging volume address the demands on the new and improved imaging techniques. The second component focuses on compatibility of the geometrical shape of the gradient relative to the shape of the main magnet, as well as the feasibility of the proposed geometrical shape to enhance patient comfort and accessibility in order the gradient system to be compatible with the largest possible spectrum of interventional and surgical applications. Since the stored magnetic energy of the gradient coil, W_m, is proportional to the fifth power of the effective radius of the structure r ($W_m \sim r^5$), any increase spacing between gradient structures, which assists in the improvement of patient comfort and accessibility, will have a negative impact on the gradient coil's field strength and slew rate with a subsequent effect the degradation of the image resolution and elongation of overall imaging time.

The initial application of biplanar gradient coil structures was intended for cylindrical bore magnets with a main field direction parallel to the surface of the planes [1,2]. The purpose of that design was to achieve proximity to the patient, while maintaining patient access and comfort. Although the biplanar structure was able to satisfy these goals, it appeared to have some significant drawbacks associated with this design concept. The most noticeable ones was the inability to design an efficient X gradient coil, and the high level of spatially asymmetric eddy currents which were the result of the variations in distance between the flat planes and the magnet's cylindrical cold shields.

When main magnet structures with vertically directed main magnetic fields were introduced, the biplanar gradient geometry became the geometry of choice [3–5], since it matches the geometrical shape of the magnet structure. There are however advantages and disadvantages associated

* Tel.: 1-330-562-1000; fax: 1-330-562-1422.

E-mail address: katrinapetropoulos@ameritech.net or lpetropoulos@usainstruments.com (L.S. Petropoulos).

0730-725X/00/$ – see front matter
PII: S0730-725X(00)00130-2

with the biplanar design. Because of the low effective radius and the large opening between the planes, the biplanar design assists on the improvement of the basic gradient properties, such as gradient strength, slew rates, gradient field linearity and uniformity, while maintaining patient comfort, reduces patient claustrophobia and enhances patient accessibility, a helpful aspect for interventional applications. In addition, due to its flat shape, the biplanar coil design reduces the hurdles on the processes which are associated with the mechanical design, the manufacturing and the maintenance of the coil. A disadvantage, which can be attributed to the biplanar structure, is that both planes have a rectangular shape while the magnet's poles have a circular cross section. In order for the gradient coil to physically fit within the magnet boundaries, the corners of the rectangle must be trimmed and thus the current of the gradient coil must be truncated at that location. The effect becomes more pronounced for actively shielded biplanar gradient structures, since the current apodization for both the primary and secondary coils is necessary in order to fit within the magnet's mechanical structure. These current truncations alter the current pattern shape on both the primary and shielding gradient coil structures and result in a significant increase of the residual eddy currents at the magnet's poles, which consequently degradates the image quality of the MRI scanner.

In this article, a new algorithm for designing finite size disc gradient coil sets compatible with vertically oriented magnetic fields is presented [6], based on the energy minimization algorithm (target field approach) as presented by Turner [7]. Specifically, the theoretical development for designing self-shielded or non-shielded transverse and/or axial disc gradient coil sets for main magnets with vertically directed fields will be presented. Numerical simulations involving Finite Element Analysis (FEA) software to evaluate the residual gradient field on the magnet poles for both the non-shielded and the self-shielded configurations is also presented. The major advantage of this disc-like gradient coil structure over the traditional biplanar design is that for the disc coils the current is physically bounded within predetermined circular cross section area. This area can be designed to match the cross sectional area of the main magnet's poles. Thus, no current truncation is necessary in order to fit the gradient set into the magnet. By avoiding the current truncation for both the primary and the secondary coils, the eddy current caused by the gradient coil at the magnet poles are minimized and the image quality is improved.

2. Theory

The geometrical configuration of the disc gradient coil set is shown in Fig. 1. The main magnetic field $\mathbf{B}_0$ is oriented along the z direction, which is perpendicular to the surface of the discs. The radius of the inner disc is denoted as R, while the gap between the two disc-like planes of the primary coil is denoted as $2a$. For the actively shielded design, the gap between the planes of the secondary discs is denoted as $2b$. In the present section, the theoretical development for the axial and transverse disc gradient coils with or without shield will be presented. An axial gradient coil configuration is defined as the gradient coil which generates a z directed field component $(G_z = \partial B_z(x, y, z)/\partial z)$ coincidental with the direction of the main magnetic field and varies linearly along the direction of the main field axis (z axis). Furthermore, a transverse gradient coil is defines as a configuration which generates a z directed field component $(G_x = \partial B_z(x, y, z)/\partial x,\ G_y = \partial B_z(x, y, z)/\partial y)$ coincidental with the direction of the main magnetic field, but varies linearly along the direction perpendicular to the main field axis (x or y axis).

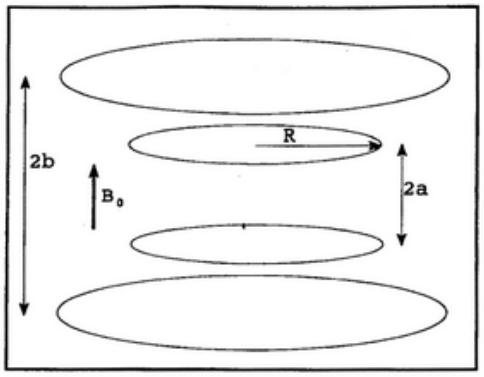

Fig. 1. Geometric configuration for a non/self-shielded Disc Gradient Coil Set. The gap between the two primary (inner) discs is denoted as $2a$, while the distance between the two shielding (outer) discs is denoted as $2b$. The radius of the disc is denoted as R.

2.1. Axial disc gradient coil set

For the axial (Z) disc gradient coil to produce G_z, its current density is restricted to lie on the surface of each the two discs. Therefore the expression for the current density for the primary disc coil in cylindrical coordinates becomes:

$$\bar{J}^a = Q^a_m(\rho, \varphi)\hat{\Phi}\delta(|z| - a) \tag{1}$$

The z directed component of the gradient field must be antisymmetric along the Z axis, while it must be symmetric along the X and Y axes. These symmetry requirements indicate that the coil's current density has no angular dependence. Furthermore, the constraint that the current density is bounded inside a disc of radius R leads to Fourier series expansion[1] for $Q^a_m(\rho)$ as:

[1] An alternative way is a series expansion of $Q^a_m(\rho)$ in terms of the Bessel functions of zero and first order.

netic field along the x direction that matches a predetermined set of gradient field constraint points $B_{xc}(x_j, y_j, z_j)$ inside the desired imaging volume. In order to achieve this goal, a quadratic functional F of the current density is constructed in terms of the gradient magnetic field B_x and the stored magnetic energy as:

$$F[Q_\varphi] = W_m - \sum_{j=1}^{N} \lambda_j [B_x(\bar{r}_j) - B_{xsc}(\bar{r}_j)] \quad (26)$$

where λ_j are the Lagrange multipliers and B_{xsc} are the desired field constraint points. By minimizing the functional in equation (26) with the help of equations (24), (25), a matrix equation for the Fourier coefficients A_n is obtained as:

$$\frac{\mu_0 \pi}{2} \sum_{n'=1}^{M} A_{n'} \int_0^\infty dk [\psi_{0n}(k)\psi_{0n'}(k) + \psi_{2n}(k)\psi_{2n'}(k)] \cdot [1 + e^{-2k\alpha}][1 - e^{-2k(\delta-\alpha)}]^2 - \frac{\mu_0}{4} \sum_{j=1}^{N} \lambda_j \cos(\phi_j) \int_0^\infty dk [\psi_{2n}(k) - \psi_{0n}(k)] k e^{-k\alpha} \cosh(kz_j)[1 - e^{-2k(\delta-\alpha)}] J_1(k\rho_j) \quad (27)$$

The close matrix form of equation (27) is similar to the equations (13) and (14). The matrix solution for the coefficients A_n is given by the last expression of equation (14). Upon the determination of the Fourier coefficients A_n, the continuous current density for the primary coil is evaluated inside the surface of the disc from the equation (17). In addition, the current density of the shielding coil can be found through via a Hankel transform of the zeroth order with the help of equation (22) as:

$$Q^{\delta}_{n\varphi}(\rho) = -\int_0^\infty e^{-2\pi k(\delta-\alpha)} J_0(2\pi k\rho) k dk Q^{a}_{n\varphi}(k) \quad (28)$$

with

$$Q^{a}_{n\varphi}(k) = 2\pi \int_0^\infty J_0(2\pi k\rho) \rho d\rho Q^{a}_{n\varphi}(\rho) \quad (29)$$

Applying the stream function technique to the continuous current distributions of the primary and shielding disc coils, the respective discrete loop patterns for constant current value are generated. Given the wire patterns and using the Biot-Savart law, the B_x component of the gradient magnetic field is independently re-evaluated to ensure the accuracy of the discretization process.

Table 1
Constraint point set for the Non-Shielded Finite G_x Disc Gradient Coil

Non-Shielded G_x Disc Gradient Coil				
N	μ_i (cm)	ω_i (rad)	Z_i (cm)	$B_{xsc}(\mu_i, \omega_i, Z_i)$ (mT)
1	0.00	0.00	0.10	0.02000
2	0.00	0.00	22.5	5.04000
3	15.0	0.00	0.10	0.01770

3. Design

As a representative of the above theoretical development, the numerical results for both a non-shielded finite G_x disc and self-shielded G_x finite disc gradient coils are presented.

3.1. Non-shielded G_x disc coil

For the non-shielded G_x gradient coil, the separation between the two discs is set to $2a = 58$ cm, while the radius of the disc is set to $R = 51$ cm. Three constraint points are chosen to represent the behavior of the gradient magnetic field inside 45 cm Diameter Spherical Volume (DSV). The first constraint sets the strength of the gradient field to 20 mT/m. The second constraint specifies a 12% variation from the actual value of the gradient field along the Z gradient axis at a distance of 22.5 cm from the isocenter of the gradient field (on-axis linearity constraint). The third constraint ensures that the uniformity of the gradient magnetic field is confined within 11% from its ideal value at a radial distance of 15 cm from the gradient's isocenter (off-axis uniformity constraint). This set of constraints is shown in Table 1.

3.2. Self-shielded G_x disc gradient coil

For the actively shielded G_x disc coil, the size of the gap between the two primary discs is set to $2a = 58$ cm, while the distance between the discs of the secondary coil is set to $2b = 68$ cm. Furthermore, the radius of the disc is set to $R = 41$ cm. Once again, three constraint points are chosen to define the characteristics of the gradient magnetic field inside 45 cm DSV. The first constraint point defines a gradient field with strength of 20 mT/m near the isocenter of the disc coil. The second constraint point sets the linearity of

Table 2
Constraint point set for the Self-Shielded Finite G_x Disc Gradient Coil

Self-Shielded G_x Disc Gradient Coil				
N	μ_i (cm)	ω_i (rad)	Z_i (cm)	$B_{xsc}(\mu_i, \omega_i, Z_i)$ (mT)
1	0.10	0.00	0.00	0.02000
2	22.5	0.00	0.00	4.0050
3	0.10	0.00	20.0	0.01500

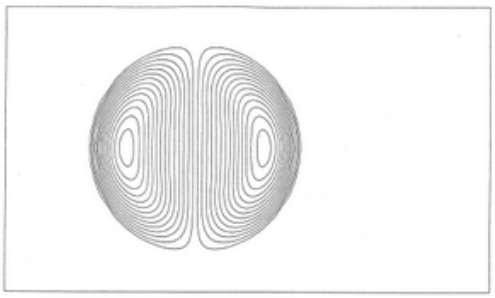

Fig. 7. One-half of the discrete current patterns for the transverse X disc coil. There are 14 Loops per quadrant with a common current per loop of 412.78 Amps.

radial behavior of the B_z component of the shielded coil's fringe field at the axial location of z = 48.5 cm. The maximum field occurs at ρ = 0 cm and is equal to 0.9 μT, while no significant spatial variation is observed.

5. Discussion

The proposed gradient coil methodology leads to an effective design procedure for minimum inductance disc gradient coils, where no apodization process was necessary in order to match the gradient structure with a round shape magnet pole. Very good numerical agreement was found between the expected (constrained) values of the gradient magnetic field and the calculated values of the gradient field at the constraint points which are generated by applying the Biot-Savart law to the discrete current pattern for both axial and transverse gradient coils. Furthermore, the flexibility of the proposed methodology for designing non-shielded and self-shielded disc gradient coils was also demonstrated. In addition, the current solution for the two disc gradient coil modalities (axial and transverse) can be easily adapted to a commercial FEA package where a full 3D harmonic analysis can be performed in order to estimate the level of eddy currents inside any desirable imaging volume.

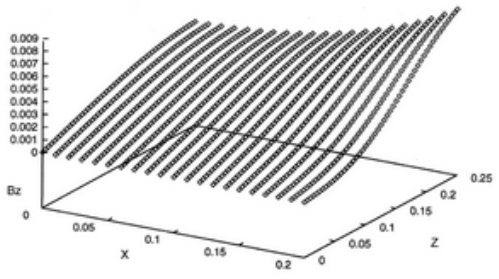

Fig. 8. Field behavior of the B_z component of the gradient field along the XZ plane for the self-shielded disc coil.

As shown in the present paper, two examples were chosen in order to demonstrate the distinct differences between a non-shielded and a self-shielded configuration. For the non-shielded configuration, the resistance and inductance of the coil are reduced significantly compared to the self-shielded design, which can be translated to the lower rise times and faster slew rates, as Table 3 illustrates. The drawback however of the non-shielded designs is the coil's high fringe field value at the vicinity of the magnet's poles. In addition to its high value, a non-constant spatial dependence is also associated with the B_z component of the gradient field. This poses a problem to an iron core magnet, where the behavior of the iron towards the magnetic field is non-linear, thus an eddy-current correction, using a gradient pre-emphasis pulse, at a certain spatial location inside the imaging volume might have a non-predicted adverse effect in a different spatial location. For this reason self-shielded designs are always preferred over non-shielded gradient structures. As Table 3 demonstrates, the value of the fringe field generated from a self-shielded design at the same axial location at the magnet's poles is almost 1000 times smaller than the value of the non-shielded design. In addition, the spatial behavior of the fringe field is almost constant. This indicates that the spatial dependence of eddy current is non-existent. The penalty paid in this case is that the coil's resistance and the inductance values are increased relative to the non-shielded design, which results in the increase of linear rise times to a full gradient strength and the consequent reduction of the coils slew rates, as Table 3 indicates.

6. Conclusions

A novel analytical methodology for designing non-shielded and actively shielded gradient coils has been presented. The purpose of the particular examples in the present paper was four fold. First, they demonstrated that no current apodization is necessary during the design disc structures suitable for magnet with vertically directed fields. Second, they were used to validate the capability of the proposed theory to design non-shielded and self-shielded disc gradient coil structures. Third, they were used to demonstrate the capability of the proposed algorithm to design axial and transverse disc gradient coil for main magnets with a main field directed along the vertical direction (perpendicular to the surface of the disc). Fourth, they demonstrated the advantages and disadvantages of an actively-shielded design versus a non-shielded design. Excellent agreement between the expected and the calculated results was found. Furthermore, a commercial FEA package by ANSYS™ was also utilized to estimate the fringe field at the vicinity of the magnet's poles. Although the proposed methodology was developed for vertical field magnets, it should aid in the development of an analogous algorithm for designing disc gradient coil for magnets with horizontally directed main fields (the main field is parallel to the surface of the disc).

Acknowledgments

Labros Petropoulos would like to thank Picker Medical Systems for their support in this project.

References

[1] Martens MA, Petropoulos LS, Brown RW, Andrews J, Morich MA, Patrick JL. Rev Sci Instr 1991;62:2639.
[2] de C. Caparelli E, Tomasi D, Panepucci H. Shielded biplaner gradient coil design. J Magn Res Imaging 1999;9:725–31.
[3] Petropoulos LS. 3rd. SMR Meeting, Poster, Nice, France, 942, 1995.
[4] Ersahin A, Hinks S, Bronskill M, Henkelman M. 4th ISMRM, Oral Presentation, New York, NY, USA, 124, 1996.
[5] Petropoulos LS, Morich MA. 6th ISMRM Meeting, Oral Presentation, Sydney, Australia, 261, 1998.
[6] Petropoulos LS. 7th ISMRM Meeting, Oral Presentation, Philadelphia, PA, USA, 471, 1999.
[7] Turner R. Minimum inductance coils. J Phys E Sci Instr 1988;21:948.